

**Existence of inelastic supernumerary nuclear rainbow in  $^{16}\text{O} + ^{12}\text{C}$  scattering**S. Ohkubo,<sup>1</sup> Y. Hirabayashi,<sup>2</sup> and A. A. Ogloblin<sup>3</sup><sup>1</sup>*Research Center for Nuclear Physics, Osaka University, Ibaraki, Osaka 567-0047, Japan*<sup>2</sup>*Information Initiative Center, Hokkaido University, Sapporo 060-0811, Japan*<sup>3</sup>*National Research Center “NRC Kurchatov Institute”, RU-123182 Moscow, Russia*

(Received 25 June 2017; published 9 August 2017)

The existence of a supernumerary nuclear rainbow in inelastic scattering is reported. This is done by studying inelastic  $^{16}\text{O}$  scattering from  $^{12}\text{C}$ , exciting the  $2^+$  (4.44 MeV) state of  $^{12}\text{C}$  and elastic scattering at the incident energies in the range 124–200 MeV, using the coupled channels method. An extended double folding potential is used. This is derived from realistic wave functions for  $^{12}\text{C}$  and  $^{16}\text{O}$  calculated with a microscopic  $\alpha$  cluster model and a finite-range density-dependent nucleon-nucleon force. Excitations to the  $2^+$  (4.44 MeV),  $3^-$  (9.64 MeV), and  $4^+$  (14.08 MeV) states of  $^{12}\text{C}$ , and the  $3^-$  (6.13 MeV) and  $2^+$  (6.92 MeV) states of  $^{16}\text{O}$  are included in the coupled channels calculations. The emergence of the supernumerary bow is understood by the properties of both the Luneburg-lens-like potential in the internal region and diffuse attraction in the outer region. The existence of a supernumerary rainbow for inelastic scattering in addition to the existence of a dynamically created secondary rainbow and a dynamically refracted primary rainbow for elastic scattering, which are not observed in meteorological rainbows, further deepens the understanding of nuclear rainbows.

DOI: [10.1103/PhysRevC.96.024607](https://doi.org/10.1103/PhysRevC.96.024607)**I. INTRODUCTION**

The existence of supernumerary bows in the inner bright side of the meteorological primary rainbow was first explained by Airy in 1938 to be caused by the wave nature of light [1–4]. The supernumerary bows also appear in the outer bright side of its secondary rainbow. The classical concept of the rainbow phenomenon was found to persist in quantum systems where the dual nature of particle and waves dominates. Hundhausen and Pauly [5] made the first observation of an atomic rainbow associated with the two supernumerary bows in the bright side of the primary rainbow for the elastic scattering of Na atoms from Hg atoms. The first observation of a nuclear rainbow was made by Goldberg *et al.* for elastic  $\alpha$  particle scattering from  $^{58}\text{Ni}$  [6]. Nuclear rainbows have been widely observed in elastic  $\alpha$  particle scattering and heavy-ion scattering under incomplete absorption, which excludes a large class of potential ambiguities of the nucleus-nucleus interaction potential [7–9]. The potential that describes rainbow scattering has been powerful in the study of the cluster structure of nuclei such as  $\alpha$  cluster structure in  $^{44}\text{Ti}$  [9] and the superdeformed  $^{16}\text{O} + ^{16}\text{O}$  cluster structure in  $^{32}\text{S}$  [10,11]. The existence of supernumerary bows in nuclear rainbow scattering, which is often called Airy structure, have been observed most clearly in heavy-ion scattering such as  $^{16}\text{O} + ^{16}\text{O}$ ,  $^{16}\text{O} + ^{12}\text{C}$ , and  $^{12}\text{C} + ^{12}\text{C}$  in the energy range between 5 and 10 MeV per nucleon [7,12–19].

Supernumerary bows in inelastic scattering, which are not expected in meteorological rainbows but are possible in quantum systems, have been observed in molecular rotational rainbows such as  $\text{Na}_2$  scattering from Ne atoms [20,21]. The nuclear rainbow in inelastic scattering has been observed and studied extensively in Refs. [7,22–29]. The existence of nuclear rainbows in inelastic scattering makes it possible to understand the interaction potential for the inelastic channels up to the internal region. In fact, the interaction potential determined in inelastic nuclear rainbow scattering has been

powerful in studying cluster structure. For example,  $\alpha$  particle condensation in the Hoyle state of  $^{12}\text{C}$  [30–33], four  $\alpha$  cluster structure in  $^{16}\text{O}$  [34], and  $\alpha + ^{16}\text{O}$  cluster structure with core excitation in  $^{20}\text{Ne}$  near the threshold energy region [35].

However, the existence of a subtle supernumerary bow in inelastic nuclear rainbow scattering has not been reported. For the most typical  $^{16}\text{O} + ^{16}\text{O}$  system the difficulty of resolution of the very close first excited  $0^+$  (6.05 MeV) and the second excited  $3^-$  (6.13 MeV) states of  $^{16}\text{O}$  hampered the identification of the Airy minimum for inelastic rainbow scattering [26]. On the other hand, for the  $^{16}\text{O} + ^{12}\text{C}$  system there is no such resolution problem for the first excited  $2^+$  state of  $^{12}\text{C}$  at 4.44 MeV. Also the Airy minima in the angular distributions are not obscured by the symmetrization, which occurs for systems with two identical bosons such as  $^{16}\text{O} + ^{16}\text{O}$  and  $^{12}\text{C} + ^{12}\text{C}$ . For  $^{16}\text{O} + ^{12}\text{C}$  there are systematic experimental data of elastic rainbow scattering over a wide range of incident energies at  $E_L = 62\text{--}1503$  MeV [13–17,27,36] and we have studied the specific mechanism of nuclear rainbows for this system such as the existence of a dynamically generated secondary bow [37], a ripple structure [38], and a dynamically refracted primary rainbow [39]. The present authors were recently able to systematically verify the existence of the Airy minimum, A1, of the primary rainbow for newly measured  $^{16}\text{O} + ^{12}\text{C}$  inelastic scattering in the energy range  $E_L = 170\text{--}281$  MeV [28]. A systematic evolution of the angular position of the Airy minimum A1 with the inverse of the center-of-mass energy was revealed. We note that the inelastic  $^{16}\text{O} + ^{12}\text{C}$  scattering measured in Ref. [40] in the energy range where the supernumerary bows appear in the elastic channel has not been paid attention from the viewpoint of a supernumerary bow. It is intriguing and challenging to investigate the existence of supernumerary bows in inelastic rainbow scattering.

The purpose of this paper is to report the existence of inelastic supernumerary nuclear rainbows in  $^{16}\text{O} + ^{12}\text{C}$  scattering in addition to the A1 and to study their Airy structure

through a coupled channels analysis of the inelastic and elastic angular distributions of differential cross sections.

## II. EXTENDED FOLDING MODEL

We study  $^{16}\text{O} + ^{12}\text{C}$  scattering with the coupled channels method using an extended double folding (EDF) model that describes all the diagonal and off-diagonal coupling potentials derived from the microscopic realistic wave functions for  $^{12}\text{C}$  and  $^{16}\text{O}$  using a density-dependent nucleon-nucleon force. The diagonal and coupling potentials for the  $^{16}\text{O} + ^{12}\text{C}$  system are calculated using the EDF model. We introduce the normalization factor  $N_R$  [8] for the real double folding potential.

$$V_{ij,kl}(\mathbf{R}) = N_R \int \rho_{ij}^{(16\text{O})}(\mathbf{r}_1) \rho_{kl}^{(12\text{C})}(\mathbf{r}_2) \times v_{NN}(E, \rho, \mathbf{r}_1 + \mathbf{R} - \mathbf{r}_2) d\mathbf{r}_1 d\mathbf{r}_2, \quad (1)$$

where  $\rho_{ij}^{(16\text{O})}(\mathbf{r})$  is the diagonal ( $i = j$ ) or transition ( $i \neq j$ ) nucleon density of  $^{16}\text{O}$  taken from the microscopic  $\alpha + ^{12}\text{C}$  cluster model wave functions calculated with the orthogonality condition model (OCM) from Ref. [41]. This model uses a realistic size parameter for the  $\alpha$  particle and for  $^{12}\text{C}$  and is an extended version of the OCM  $\alpha$  cluster model of Ref. [42], which reproduces almost all the energy levels well up to  $E_x \approx 13$  MeV and the electric transition probabilities for  $^{16}\text{O}$ . We take into account the important transition densities

available in Ref. [41], i.e.,  $g.s \leftrightarrow 3^-$  (6.13 MeV) and  $2^+$  (6.92 MeV) in addition to all the diagonal densities.  $\rho_{kl}^{(12\text{C})}(\mathbf{r})$  represents the diagonal ( $k = l$ ) or transition ( $k \neq l$ ) nucleon density of  $^{12}\text{C}$  calculated using the microscopic three  $\alpha$  cluster model of the resonating group method [43]. This model reproduces the structure of  $^{12}\text{C}$  well and the wave functions have been checked against many experimental data, including charge form factors and electric transition probabilities [43]. In the coupled channels calculations we take into account the  $0_1^+$  (0.0 MeV),  $2^+$  (4.44 MeV),  $3^-$  (9.64 MeV), and  $4^+$  (14.08 MeV) states of  $^{12}\text{C}$ . The mutual excitation channels in which both  $^{12}\text{C}$  and  $^{16}\text{O}$  are excited simultaneously are not included. For the effective interaction  $v_{NN}$  we use the DDM3Y-FR interaction [44], which takes into account the finite-range exchange effect [45]. An imaginary potential (nondeformed) is introduced phenomenologically for all the diagonal potentials to take into account the effect of absorption due to other channels, which was successful in the recent coupled channels studies of  $^{16}\text{O} + ^{12}\text{C}$  rainbow scattering [28,37,38]. Off-diagonals are assumed to be real. Coulomb excitation is included.

## III. COUPLED CHANNELS ANALYSIS AND SUPERNUMERARY BOW IN INELASTIC SCATTERING

In Fig. 1 angular distributions of elastic and inelastic  $^{16}\text{O} + ^{12}\text{C}$  scattering at  $E_L = 124\text{--}200$  MeV, calculated using the

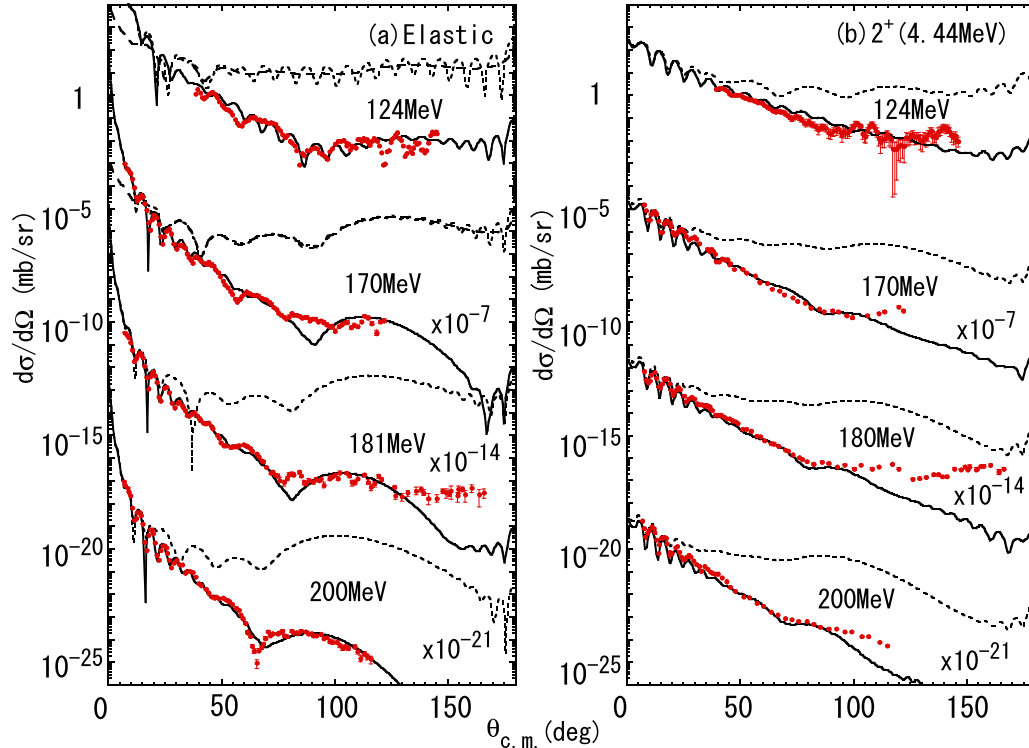


FIG. 1. Angular distributions in  $^{16}\text{O} + ^{12}\text{C}$  scattering at  $E_L = 124, 170, 181$  (180), and 200 MeV calculated with the potentials in Table I using the coupled channels method (solid lines) are compared with the experimental data (filled circles with vertical error bars) taken from Refs. [16,28,40], (a) elastic scattering and (b) inelastic scattering to the  $2^+$  state of  $^{12}\text{C}$ . The dotted lines are calculated by switching off the imaginary potentials in Table I in (a) and only the imaginary potentials in the  $2^+$  channel are switched off in (b). In (a) far-side components calculated by switching off the imaginary potentials are displayed by with dashed lines for  $E_L = 124$  and 170 MeV.

TABLE I. The volume integral per nucleon pair  $J_V$  of the DF potential and the imaginary potential parameters (strength  $W$ , radius  $R$  and diffuseness  $a$ ) used in the coupled channels calculations are displayed.  $J_V$  is given only for the elastic  $^{16}\text{O}(\text{g.s.})\text{-}^{12}\text{C}(\text{g.s.})$  channel.

$E_L$ (MeV)	$J_V$ (MeV fm <sup>3</sup> )	$W$ (MeV)	$R$ (fm)	$a$ (fm)
124	306.1	16	5.6	0.30
170	296.9	17	5.6	0.55
181	294.9	17	5.6	0.55
200	291.6	18	5.6	0.60

coupled channels method, are displayed in comparison with the experimental data. We take  $N_R = 0.97$  and the imaginary potentials given in Table I are used for all the channels. In Fig. 1(a) the agreement of the calculated angular distributions for elastic scattering with the experimental data is comparable to Ref. [28]. The energy evolution of the angles of the Airy minimum in the angular distributions in elastic scattering is consistent with that studied with the single-channel optical potential model in the lower-energy region 62–124 MeV in Ref. [14,15] and in the higher-energy region 132–260 MeV in Ref. [16]. In Fig. 1(a) we note that for the coupled channels calculations in which the imaginary potentials are switched off, supernumerary bows with higher-order Airy minima are seen at angles smaller than the A1 minima. The supernumerary

bows with Airy minima up to A5 (order five) for elastic scattering have been observed at lower energies between 85 MeV and 132 MeV by Szilner *et al.* [15]. They observed the A2, A3, and A4 minima at around  $\theta_{\text{c.m.}} = 94^\circ$ ,  $60^\circ$ , and  $40^\circ$  in the angular distribution for  $E_L = 124$  MeV and at around  $81^\circ$ ,  $58^\circ$ , and  $37^\circ$  for  $E_L = 132$  MeV, respectively [15]. Ogloblin *et al.* [16] observed the A2 and A3 minima at around  $55^\circ$  and  $39^\circ$  at  $E_L = 170$  MeV, respectively. At 200 and 230 MeV, only the A2 minimum was observed at around  $45^\circ$  and  $35^\circ$ , respectively [16]. Above this energy a higher-order Airy structure greater than A2 has not been observed, although the A1 appears up to 608 MeV [16]. Regarding the inelastic scattering to the  $2^+$  state in Fig. 1(b), the characteristic features of the experimental angular distributions are reproduced well by the calculations. In the angular distributions at 170 MeV calculated by switching off only the imaginary potential in the channel of the  $2^+$  state of  $^{12}\text{C}$ , we observe a minimum at around  $60^\circ$  faintly in addition to the Airy minimum A1 at around  $90^\circ$  reported in Ref. [28]. A similar minimum is seen clearly at 124 MeV.

Since there are no inelastic scattering experimental data available between 170 and 124 MeV, in order to facilitate identification of the order of the Airy minima at 124 MeV, the energy evolution of the Airy minimum between 170 and 124 MeV is displayed in intervals of 10 MeV in Fig. 2. In order that the Airy minima in Fig. 1(a) in elastic scattering can be seen clearly, in Fig. 2(a) the far-side components of the

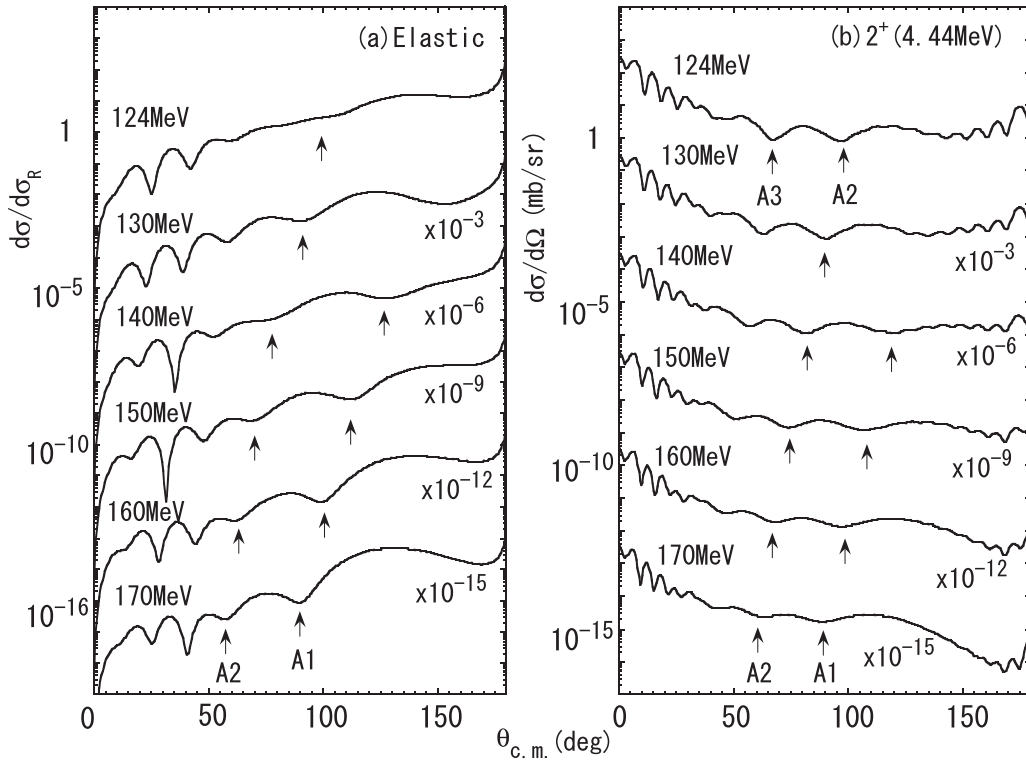


FIG. 2. Energy evolution of the angular distributions in  $^{16}\text{O} + ^{12}\text{C}$  scattering calculated by switching off the imaginary potential for  $E_L = 170\text{--}124$  MeV at intervals of 10 MeV using the coupled channels method are displayed for (a) elastic (ratio to Rutherford scattering) and (b) inelastic scattering to the  $2^+$  state of  $^{12}\text{C}$ . For the inelastic scattering in (b) only the imaginary potential in the  $2^+$  channel is switched off. In (a) the solid lines represent the far-side components. The labels A1, A2, and A3 indicate the position of the Airy minimum of the order one, two, and three, respectively.

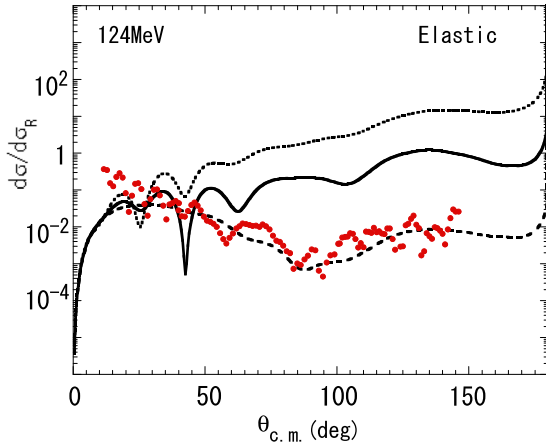


FIG. 3. The far-side contribution of the angular distribution (ratio to Rutherford scattering) in  $^{16}\text{O} + ^{12}\text{C}$  elastic scattering at  $E_L = 124$  MeV calculated using the coupled channels method and the experimental data (filled circles) [40]. The dashed line, solid line and the dotted line represent the coupled channels calculation with  $W = 16$  (Table I),  $W = 4$ , and  $W = 0$ , respectively.

cross sections (in ratio to Rutherford scattering) calculated by switching off the imaginary potential are displayed. In Fig. 2(b) we can identify the Airy minimum A2 at around  $63.5^\circ$  for  $E_L = 170$  MeV and  $97.5^\circ$  for  $E_L = 124$  MeV in the angular distributions calculated by switching off only the imaginary potential in the  $^{12}\text{C}(2^+)$  channel. At 124 MeV the Airy minimum A3 is seen at  $67.5^\circ$ . The minimum at  $50^\circ$  in the angular distributions of inelastic scattering at 200 MeV calculated by switching off the imaginary potentials in Fig. 1(b) is found to be A2, which is faintly seen at around  $50^\circ$  in the experimental data.

In Fig. 3 the far-side contribution to angular distributions for elastic scattering at 124 MeV is displayed for different imaginary potential strengths. The position of the Airy minima in the coupled channel calculations does not change for  $W = 0, 4$  and  $16$  MeV. When absorption is switched off ( $W = 0$ ), the Airy minima appear in the far-side scattering angular distributions, A2, A3, and A4 at  $104^\circ$ ,  $62^\circ$ , and  $42.5^\circ$ , respectively. By increasing absorption to  $W = 4$ , the A2, A3, and A4 minima appear clearly at  $103^\circ$ ,  $62^\circ$ , and  $42^\circ$ , respectively. Despite absorption, the supernumerary bows in elastic scattering survive at 124 MeV.

#### IV. DISCUSSION

The mechanism and the logic that the supernumerary bow survives in inelastic scattering are quite similar to elastic scattering. In fact, the A2, A3, and A4 Airy minima at the angles around  $97.5^\circ$ ,  $67.5^\circ$ , and  $46^\circ$  in the angular distributions at 124 MeV calculated by switching off the absorption only in the  $^{12}\text{C}(2^+)$  channel are obscured when  $W$  is increased to  $W = 16$ . However, their angular positions are slightly altered similar to the elastic scattering case as shown in Fig. 1. The minimum at around  $95^\circ$  in the experimental data of inelastic scattering, which is very close to the Airy minimum A2 of the

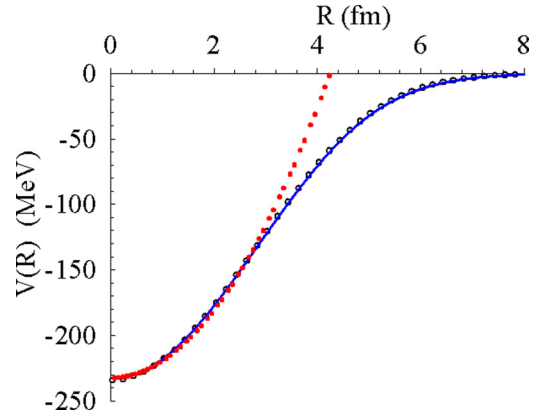


FIG. 4. Comparison of the  $^{16}\text{O} + ^{12}\text{C}$  folding potential for the inelastic channel to the  $^{12}\text{C}(2^+)$  state (open circles) at 124 MeV with that for elastic channel (blue solid line) and a Luneburg lens potential (red filled circles) with  $V_0 = 233$  MeV and  $R_0 = 4.26$  fm. The Luneburg lens potential is given by [46]  $V(R \leq R_0) = V_0(R^2/R_0^2 - 1)$  and  $V(R > R_0) = 0$  with  $R_0$  being the size of the lens.

experimental data in elastic scattering, is thus assigned to be the higher-order Airy minimum A2.

The similarity of the logic of the emergence of the supernumerary Airy structure in inelastic scattering to that in elastic scattering can be understood by looking at the real potentials that cause strong refraction and astigmatism due to the diffuse surface of the nuclear potential. In Fig. 4 the folding potential for the inelastic  $^{16}\text{O}(\text{g.s.}) - ^{12}\text{C}(2^+)$  channel at 124 MeV used in the coupled channels calculations in Fig. 1 is compared with that for elastic scattering and a Luneburg lens potential. We see that the potential for the inelastic channel (open circles) with  $J_V = 303$  MeVfm<sup>3</sup> is almost indistinguishable from the elastic channel (solid line) with  $J_V = 306$  MeVfm<sup>3</sup>. We also clearly see that the potential for the inelastic channel is similar to a Luneburg lens potential in the internal region. Notch test calculations, in which the diagonal real potentials both in the elastic and inelastic channels are slightly modified by adding a peaked attraction located at  $R = R_1$  with a small width  $a_1 = 0.15$  fm, show that the angular distributions at angles where the Airy structure appears are sensitive to the internal region,  $R_1 < 3$  fm, of the potential not only in elastic channel but also in inelastic channel. A notch potential shifts the position of the Airy minimum in the angular distributions. The emergence of the nuclear rainbow with a supernumerary bow is due the properties of both the Luneburg-lens-like potential in the internal region and the diffuse attraction in the outer region of the nuclear potential as in elastic scattering [46].

In Fig. 5 the energy evolution of the angular position of the Airy minimum for elastic scattering and inelastic scattering are displayed as a function of the inverse center-of-mass (c.m.) energies. The Airy minimum A1 for elastic and inelastic scattering to the  $2^+$  state of  $^{12}\text{C}$  at the higher energies  $E_L = 260$  and  $281$  MeV determined in Ref. [28] are also included. The Airy minimum A1 for inelastic scattering is slightly shifted backward compared with that for elastic scattering. This backward shift is considered to be caused by the excitation energy effect as discussed in Ref. [22]. This backward shift is

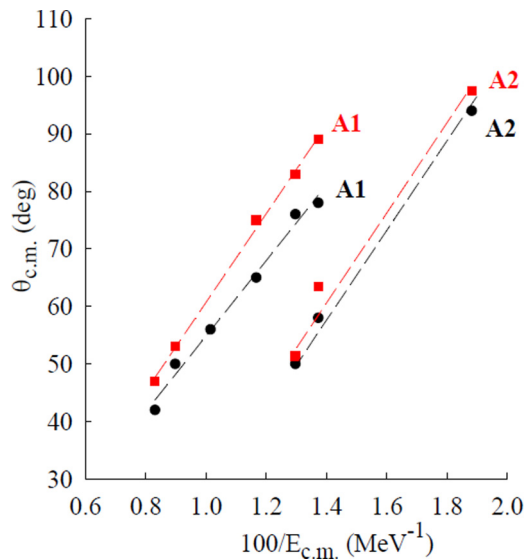


FIG. 5. The positions of the Airy minimum observed in inelastic scattering to the  $2^+$  state of  $^{12}\text{C}$  (filled squares) and elastic scattering (filled circles) of  $^{16}\text{O} + ^{12}\text{C}$  are displayed as a function of the inverse center-of-mass (c.m.) energies. The labels A1 and A2 indicate the order of the Airy minima. The lines are to guide the eye.

small for A2. The positions of the Airy minima A2 for inelastic scattering vary approximately linearly with c.m. energy similar to those for elastic scattering [17]. This seems to support the assignment of the higher-order Airy minimum for inelastic scattering to the  $2^+$  state of  $^{12}\text{C}$ .

Finally we mention that the present model with an EDF interaction enables us to study cluster structure with the  $^{16}\text{O} + ^{12}\text{C}(2^+)$  configuration at lower energies and the emergence of a nuclear rainbow in inelastic scattering in a unified way. This is a subject for future research.

## V. SUMMARY

To summarize, we have reported the existence of a supernumerary bow in inelastic scattering by investigating  $^{16}\text{O} + ^{12}\text{C}$  scattering to the  $2^+$  (4.44 MeV) state of  $^{12}\text{C}$ . The systematic analysis of rainbow scattering at  $E_L = 124\text{--}200$  MeV was undertaken using an extended double folding model derived from the realistic wave functions for  $^{12}\text{C}$  and  $^{16}\text{O}$  calculated with a microscopic  $\alpha$  cluster model with a finite-range density-dependent nucleon-nucleon force. In the coupled channels calculations couplings to the  $0_1^+$  (0.0 MeV),  $2^+$  (4.44 MeV),  $3^-$  (9.64 MeV), and  $4^+$  (14.08 MeV) states of  $^{12}\text{C}$  and the  $0_1^+$  (0.0 MeV), the  $3^-$  (6.13 MeV) and  $2^+$  (6.92 MeV) states of  $^{16}\text{O}$  were taken into account. The coupled channels analysis made it possible to assign the emergence of the higher-order Airy minimum and the known A1 minimum in the inelastic scattering cross sections to the first  $2^+$  state of  $^{12}\text{C}$ . The existence of a supernumerary rainbow for the inelastic channel of nuclear rainbow scattering in addition to the existence of a dynamically created secondary bow [37] and a dynamically refracted primary bow [39] for elastic scattering, which are not expected in meteorological rainbows, deepen the understanding of rainbows under strong interactions.

## ACKNOWLEDGMENTS

Two of the authors (S.O. and Y.H.) would like to thank the Yukawa Institute for Theoretical Physics, Kyoto University for the hospitality extended during stays where part of this work was done. One of the authors (S.O.) is grateful to Dr. Paul Suckling for careful reading of the manuscript and useful comments. We thank Professor Masayasu Kamimura for providing the newly calculated transition densities of  $^{12}\text{C}$  and Professor Florent Haas for the tabulated form of the numerical data of Ref. [40].

- 
- [1] H. M. Nussenzveig, *Sci. Am.* **236**, 116 (1977).  
 [2] G. B. Airy, *Trans. Cambridge Philos. Soc.* **6**, 379 (1838).  
 [3] J. D. Jackson, *Phys. Rep.* **320**, 27 (1999).  
 [4] J. A. Adam, *Phys. Rep.* **56**, 229 (2002).  
 [5] E. Hundhausen and H. Pauly, *Z. Phys.* **187**, 305 (1965).  
 [6] D. A. Goldberg, S. M. Smith, and G. F. Burdzyk, *Phys. Rev. C* **10**, 1362 (1974).  
 [7] D. T. Khoa, W. von Oertzen, H. G. Bohlen, and S. Ohkubo, *J. Phys. G* **34**, R111 (2007).  
 [8] M. E. Brandan and G. R. Satchler, *Phys. Rep.* **285**, 143 (1997); and references therein.  
 [9] F. Michel, S. Ohkubo, and G. Reidemeister, *Prog. Theor. Phys. Suppl.* **132**, 7 (1998); and references therein.  
 [10] S. Ohkubo and K. Yamashita, *Phys. Rev. C* **66**, 021301(R) (2002).  
 [11] S. Ohkubo, *Proceedings of Symposium on Nuclear Clusters: From Light Exotic to Superheavy Nuclei*, edited by J. Jolos and W. Scheid (EP Systema, Debrecen, 2003), p.161; S. Ohkubo, *Heavy Ion Phys.* **18**, 287 (2003).  
 [12] M. P. Nicoli, F. Haas, R. M. Freeman, N. Aissaoui, C. Beck, A. Elanique, R. Nouicer, A. Morsad, S. Szilner, Z. Basrak, M. E. Brandan, and G. R. Satchler, *Phys. Rev. C* **60**, 064608 (1999).  
 [13] A. A. Ogloblin, Dao T. Khoa, Y. Kondō, Yu. A. Glukhov, A. S. Dem'yanova, M. V. Rozhkov, G. R. Satchler, and S. A. Goncharov, *Phys. Rev. C* **57**, 1797 (1998).  
 [14] M. P. Nicoli, F. Haas, R. M. Freeman, S. Szilner, Z. Basrak, A. Morsad, G. R. Satchler, and M. E. Brandan, *Phys. Rev. C* **61**, 034609 (2000).  
 [15] S. Szilner, M. P. Nicoli, Z. Basrak, R. M. Freeman, F. Haas, A. Morsad, M. E. Brandan, and G. R. Satchler, *Phys. Rev. C* **64**, 064614 (2001).  
 [16] A. A. Ogloblin, Y. A. Glukhov, V. Trzaska, A. S. Dem'yanova, S. A. Goncharov, R. Julin, S. V. Klebnikov, M. Mutterer, M. V. Rozhkov, V. P. Rudakov, G. P. Tiorin, D. T. Khoa, and G. R. Satchler, *Phys. Rev. C* **62**, 044601 (2000).  
 [17] A. A. Ogloblin, S. A. Goncharov, Yu. A. Glukhov, A. S. Dem'yanova, M. V. Rozhkov, V. P. Rudakov, and W. H. Trzaska, *Phys. At. Nucl.* **66**, 1478 (2003).  
 [18] R. G. Stokstad, R. M. Wieland, G. R. Satchler, C. B. Fulmer, D. C. Hensley, S. Raman, L. D. Rickertsen, A. H. Snell, and P. H. Stelson, *Phys. Rev. C* **20**, 655 (1979).  
 [19] F. Michel and S. Ohkubo, *Eur. Phys. J. A* **19**, 333 (2004).  
 [20] U. Hefter, P. L. Jones, A. Mattheus, J. Witt, K. Bergmann, and R. Schinke, *Phys. Rev. Lett.* **46**, 915 (1981).

- [21] E. Gottwald, K. Bergmann, and R. Schinke, *J. Chem. Phys.* **86**, 2685 (1987).
- [22] F. Michel and S. Ohkubo, *Phys. Rev. C* **70**, 044609 (2004); *Nucl. Phys. A* **738**, 231 (2004).
- [23] H. G. Bohlen, M. R. Clover, G. Ingold, H. Lettau, and W. von Oertzen, *Z. Phys. A* **308**, 121 (1982).
- [24] H. G. Bohlen, X. S. Chen, J. G. Cramer, P. Fröbrich, B. Gebauer, H. Lettau, A. Miczaika, W. von Oertzen, R. Ulrich, and T. Wilpert, *Z. Phys. A* **322**, 241 (1985).
- [25] H. G. Bohlen, E. Stiliaris, B. Gebauer, W. von Oertzen, M. Wilpert, Th. Wilpert, A. Ostrowski, Dao T. Khoa, A. S. Dem'yanova, and A. A. Ogloblin, *Z. Phys. A* **346**, 189 (1993).
- [26] D. T. Khoa, H. G. Bohlen, W. von Oertzen, G. Bartnitzky, A. Blazevic, F. Nuoffer, B. Gebauer, W. Mittig, and P. Roussel-Chomaz, *Nucl. Phys. A* **759**, 3 (2005).
- [27] M. E. Brandan, A. Menchaca-Rocha, M. Buenerd, J. Chauvin, P. DeSaintignon, G. Duhamel, D. Lebrun, P. Martin, G. Perrin, and J. Y. Hostachy, *Phys. Rev. C* **34**, 1484 (1986).
- [28] S. Ohkubo, Y. Hirabayashi, A. A. Ogloblin, Yu. A. Gloukhov, A. S. Dem'yanova, and W. H. Trzaska, *Phys. Rev. C* **90**, 064617 (2014).
- [29] F. Michel and S. Ohkubo, *Phys. Rev. C* **72**, 054601 (2005).
- [30] S. Ohkubo and Y. Hirabayashi, *Phys. Rev. C* **70**, 041602(R) (2004).
- [31] S. Ohkubo and Y. Hirabayashi, *Phys. Rev. C* **75**, 044609 (2007).
- [32] T. L. Belyaeva, A. N. Danilov, A. S. Dem'yanova, S. A. Goncharov, A. A. Ogloblin, and R. Perez-Torres, *Phys. Rev. C* **82**, 054618 (2010).
- [33] Sh. Hamada, Y. Hirabayashi, N. Burtabayev, and S. Ohkubo, *Phys. Rev. C* **87**, 024311 (2013).
- [34] S. Ohkubo and Y. Hirabayashi, *Phys. Lett. B* **684**, 127 (2010).
- [35] Y. Hirabayashi and S. Ohkubo, *Phys. Rev. C* **88**, 014314 (2013).
- [36] W. H. Trzaska, *Phys. At. Nucl.* **65**, 725 (2002).
- [37] S. Ohkubo and Y. Hirabayashi, *Phys. Rev. C* **89**, 051601(R) (2014).
- [38] S. Ohkubo and Y. Hirabayashi, *Phys. Rev. C* **89**, 061601(R) (2014).
- [39] S. Ohkubo and Y. Hirabayashi, *Phys. Rev. C* **94**, 034601 (2016).
- [40] S. Szilner, F. Haas, Z. Basrak, R. M. Freeman, A. Morsad, and M. P. Nicoli, *Nucl. Phys. A* **779**, 21 (2006); S. Szilner *et al.*, IAEA Database EXFOR, <http://www-nds.iaea.org/exfor/>.
- [41] S. Okabe, in *Tours Symposium on Nuclear Physics II*, edited by H. Utsunomiya *et al.* (World Scientific, Singapore, 1995), p. 112.
- [42] Y. Suzuki, *Prog. Theor. Phys.* **55**, 1751 (1976); **56**, 111 (1976).
- [43] M. Kamimura, *Nucl. Phys. A* **351**, 456 (1981).
- [44] A. M. Kobos, B. A. Brown, P. E. Hodgson, G. R. Satchler, and A. Budzanowski, *Nucl. Phys. A* **384**, 65 (1982); A. M. Kobos, B. A. Brown, R. Lindsay, and G. R. Satchler, *ibid.* **425**, 205 (1984); G. Bertsch, J. Borysowicz, H. McManus, and W. G. Love, *ibid.* **284**, 399 (1977).
- [45] D. T. Khoa, W. von Oertzen, and H. G. Bohlen, *Phys. Rev. C* **49**, 1652 (1994).
- [46] F. Michel, G. Reidemeister, and S. Ohkubo, *Phys. Rev. Lett.* **89**, 152701 (2002).